Available online at www.sciencedirect.com

ScienceDirect

Biochimica et Biophysica Acta 1767 (2007) 1401–1411

Biochimica et Biophysica Acta BBA

www.elsevier.com/locate/bbabio

Identification of amino acid residues participating in the energy coupling and proton transport of *Streptomyces coelicolor* A3(2) H^+-pyrophosphatase

Megumi Hirono, Yoichi Nakanishi, Masayoshi Maeshima *

Laboratory of Cell Dynamics, Graduate School of Bioagricultural Sciences, Nagoya University, Nagoya 464-8601, Japan

Received 7 July 2007; received in revised form 5 September 2007; accepted 20 September 2007
Available online 29 September 2007

Abstract

The H^+-translocating inorganic pyrophosphatase is a proton pump that hydrolyzes inorganic pyrophosphate. It consists of a single polypeptide with 14–17 transmembrane domains (TMs). We focused on the third quarter region of *Streptomyces coelicolor* A3(2) H^+-pyrophosphatase, which contains a long conserved cytoplasmic loop. We assayed 1520 mutants for pyrophosphate hydrolysis and proton translocation, and selected 34 single-residue substitution mutants with low substrate hydrolysis and proton-pump activities. We also generated 39 site-directed mutant enzymes and assayed their activity. The mutation of 5 residues in TM10 resulted in low energy-coupling efficiencies, and mutation of conserved residues Thr^{409}, Val^{411}, and Gly^{414} showed neither hydrolysis nor pumping activity. The mutation of six, five, and four residues in TM11, 12, and 13, respectively, gave a negative effect. Phe^{388}, Thr^{389}, and Val^{396} in cytoplasmic loop *i* were essential for efficient H^+ translocation. Ala^{436} and Pro^{560} in the periplasmic loops were critical for coupling efficiency. These low-efficiency mutants showed dysfunction of the energy-conversion and/or proton-translocation activity. The energy efficiency was increased markedly by the mutation of two and six residues in TM9 and 12, respectively. These results suggest that TM10 is involved in enzyme function, and that TM12 regulate the energy-conversion efficiency. H^+-pyrophosphatase might involve dynamic linkage between the hydrophilic loops and TMs through the central half region of the enzyme.

Keywords: Energy coupling; H^+-pyrophosphatase; Random mutagenesis; Proton pump

1. Introduction

Proton pumps convert the energy of high-energy compounds into the active transport of protons across biomembranes. They play two physiological roles: pH regulation and the formation of proton-motive forces in their membranes. The simplest of these pumps is the H^+-translocating inorganic pyrophosphatase (H^+-PPase), which consists of a single polypeptide of ~80 kDa [1]. H^+-PPases are found in plants, parasitic and free-living protozoa, and some eubacteria and archaebacteria [2–7]. In prokaryotes, such as *Rhodospirillum rubrum* [2,8,9], *Pyrobaculum aerophilum* [10], and *Agrobacterium tumefaciens* [11], the enzyme generates a proton gradient across the plasma membrane and the membranes of acidocalcisomes. Its physiological role has also been investigated in plants [12–16] and other organisms [8,17–19].

The H^+-PPase enzyme is an excellent model for research into the coupling between pyrophosphate (PPi) hydrolysis and active proton transport because it consists of a single protein and has a simple substrate. Site-directed mutagenesis revealed several functional motifs in the H^+-PPases of *Arabidopsis thaliana* [4,20,21], *Vigna radiata* [22–24], *R. rubrum* [25,26], *Carboxydothermus hydrogenoformans* [27], and *Streptomyces coelicolor* A3(2) [28–31]. Membrane topological analysis showed that all the common functional motifs for Mg-PPi binding and PPi hydrolysis are faced to the cell cytosol, which is where the substrate is generated [28].

In the present study, we investigated how H^+-PPase couples the hydrolysis of PPi with the active transport of protons across the membrane. As a model enzyme we used *S. coelicolor* A3(2) H^+-PPase (ScPP), which comprises 794 amino acids and 17 transmembrane domains (TMs) [28]. To examine the coupling

Abbreviations: DTT, dithiothreitol; H^+-PPase, H^+-translocating inorganic pyrophosphatase; ScPP, *S. coelicolor* A3(2) H^+-PPase; TM, transmembrane domain; WT, wild type

* Corresponding author. Tel./fax: +81 52 789 4096.
E-mail address: maeshima@agr.nagoya-u.ac.jp (M. Maeshima).

0005-2728/$ - see front matter © 2007 Elsevier B.V. All rights reserved.
doi:10.1016/j.bbabio.2007.09.007

Table 1
Summary of random mutants of *S. coelicolor* A3(2) H^+-PPases

Mutant	Mutation	Result	Mutant	Mutation	Result
F388L	1162T→C	F→L	P473L	1418C→T	P→L
F388S	1163T→C	F→S	S475P	1423T→C	S→P
T389A	1165A→G	T→A	A478T	1374G→A	Silent
V396A	1187T→C	V→A		1432G→A	A→T
S402P	1204T→C	S→P	G480D	1439G→A	G→D
I415T	1244T→C	I→T	L496P	1487T→C	L→P
L419P	1256T→C	L→P	D500G	1499A→G	D→G
S421G	1261A→G	S→G	T510I	1529C→T	T→I
V423I	1267G→A	V→I	K511E	1531A→G	K→E
Y424C	1218T→C	Silent		1563A→G	Silent
	1271A→G	Y→C	T517I	1550C→T	T→I
A436P	1306G→C	A→P	A524V	1571C→T	A→V
L438P	1313T→C	L→P	L525S	1574T→C	L→S
L448P	1323A→G	Silent	Y529C	1586A→G	Y→C
	1343T→C	L→P	D556G	1667A→G	D→G
F449L	1345T→C	F→L	F574L	1242T→C	Silent
L453S	1358T→C	L→S		1720T→G	F→L
T460I	1379C→T	T→I	L575Q	1724T→A	L→Q
D469G	1406A→G	D→G	L579P	1736T→C	L→P
F471S	1412T→C	F→S			

Random mutagenesis generated 1520 mutants of ScPP. In total, 34 mutants with low PPase activity, low H^+-pump activity or low energy-coupling efficiency were selected from the random mutants (see text for details). DNAs for the mutants were sequenced individually. Mutation sites including silent mutations are listed.

mechanism and the structural–functional relationship, we separated the primary structure into four parts and constructed ScPP mutant libraries for each part using random mutagenesis. We focused on the third quarter, which consists of TM10 to TM13 and two conserved motifs in a hydrophilic loop. We prepared a random mutant library of H^+-PPase, and surveyed mutants with a low coupling efficiency between PPi hydrolysis and proton pumping. We also prepared site-directed mutants of H^+-PPase and determined the effect of mutating residues in the TMs and hydrophilic loops on enzyme activity and energy coupling. The structural and functional significance of these mutations is discussed in relation to the energy-transducing mechanism.

2. Materials and methods

2.1. Random mutagenesis of the third quarter of sScPP

A *ScPP* gene was isolated from DNA of laboratory strain of *S. coelicolor* A3(2) as described previously [31] and a synthetic *ScPP* gene was prepared without changing its amino acid sequence as described previously [28]. A hexahistidine (His_6) tag was added to the carboxyl-terminus to detect the ScPPs protein by immunoblotting. *ScPP* constructs in pYN309 were introduced into *Escherichia coli* strain BLR(DE3)pLysS (Novagen, Madison, WI) [31].

A random mutant library of *sScPP* was constructed using PCR-based random mutagenesis (error-prone PCR) according to the method described previously [22, 31]. Briefly, the third quarter region of ScPP (amino acids Leu^{384} to Arg^{586}) was subjected to random mutagenesis. PCR was carried out in a 50-μl solution containing 10 ng pYN025 plasmid, 10 mM Tris–HCl [pH 8.3], 50 mM KCl, 0.001% gelatin, 2.5 mM $MgCl_2$, 0.1 mM dATP, 0.1 mM dCTP, 1 mM dGTP, 1 mM dTTP, 2.5 U AmpliTaq DNA polymerase (Perkin Elmer, Wellesley, MA), and 250 nM primers (forward primer, 5′-AGTCTGGTGATCCTCG-TATCCTTGC-3′; reverse primer, 5′- CCATAATACCTGGACGTTCGCG-GAA-3′). The PCR conditions were 18 cycles of 30 s at 95 °C, 60 s at 55 °C, and 3 min at 72 °C. The resulting PCR fragments were digested and inserted into the *Mun*I–*Pst*I site of pYN316. The plasmids generated were amplified in *E. coli* DH5α and used as a random mutant library (total transformant number = 9.7×10^4). The mutation frequency of the library was determined to be 0.4 nucleotide change per clone by DNA sequencing. The amplified library DNA was purified and introduced into an *E. coli* expression host BLR(DE3) pLysS K128I [28].

2.2. Site-directed mutagenesis of ScPP

Mutant derivatives of ScPP were generated with a QuikChange site-directed mutagenesis kit (Stratagene, La Jolla, CA) according to the method of Kirsh and Joly [32] as described previously [22,28,31]. The nucleotide sequences of the mutants were confirmed by DNA sequencing.

2.3. ScPP expression and preparation of E. coli membrane

Expression of ScPP in *E. coli* cells and preparation of membrane from the cells were carried out described previously [31]. The obtained membrane fractions were suspended in 10 mM Tris–Mes [pH 7.3], 1 mM DTT, 1 mM $MgCl_2$, 100 mM KCl, 0.15 M sucrose, and 0.5 mM phenylmethanesulfonyl fluoride, and used for enzyme assay and immunoblotting.

2.4. Protein and enzyme assays

The protein content was quantified using the Bradford method [33]. PPi hydrolysis was measured at 30 °C as described previously [5,34] with the exception that the concentration of Na_4PPi was 0.4 mM. The actual substrate for H^+-PPase is the Mg_2PPi complex [35] and the concentration of Mg_2PPi under the assay condition was calculated to be 71 μM, which is sufficient for expression of full activity of ScPP [34]. PPi-dependent H^+-transport activity was measured as the initial rate of fluorescence quenching of acridine orange at 25 °C as described previously [5,36,37]. The enzyme reaction was initiated by adding 0.4 mM Na_4PPi [31].

2.5. SDS-PAGE and immunoblotting

Proteins were separated by SDS-PAGE on 12% gels and transferred to a polyvinylidene difluoride membrane (Millipore, Billerica, MA). Immunoblotting was carried out using horseradish peroxidase-linked protein A and ECL Western blotting detection reagents (GE Healthcare, Bio-sciences, Piscataway, NJ). The polyclonal antibodies against a hexahistidine tag (anti-His_6 antibodies; MBL Co., Nagoya, Japan) were used for quantitation of ScPP mutant proteins in the *E. coli* membrane fractions.

3. Results

3.1. Screening of the random ScPP mutant library

We examined the effect of amino acid replacement in the third quarter of ScPP, which comprises 203 residues from Leu^{384} to Arg^{586}. This region contains four hydrophilic loops

Fig. 1. Expression levels and enzyme activities of random mutants of ScPP. Membrane vesicles were prepared from *E. coli* cells expressing WT ScPP and mutants with single-residue replacements. (A) Membranes (5 μg per lane) were subjected to immunoblotting with anti-His_6 antibodies (upper panel). The intensities of the immunostained bands were quantified and are expressed relative to that of WT (lower panel). (B) PPase activity of the mutants is expressed relative to that of WT (87 nmol PPi/min/mg protein). (C) H^+-pump activities of WT and mutants were measured and are expressed relative to that of WT (103%Δ*F*/min/mg protein). (D) Coupling efficiency was calculated as the ratio of H^+-pump activity to PPase activity, and is expressed relative to that of WT. Mutant ScPPs are categorized into "no activity" (black circles), "pump-less" (open circles), and "loose-coupling" mutants (grey circles; see text for details).

with conserved segments and four TMs (TM10–TM13). The accumulation of ScPP protein and enzyme activity were assessed in 1520 ScPP mutants. Membrane fractions were individually assayed for PPi hydrolysis (PPase) and PPi-dependent H^+-pump activities. Most mutants had full PPase activity, although some had low or negligible activity.

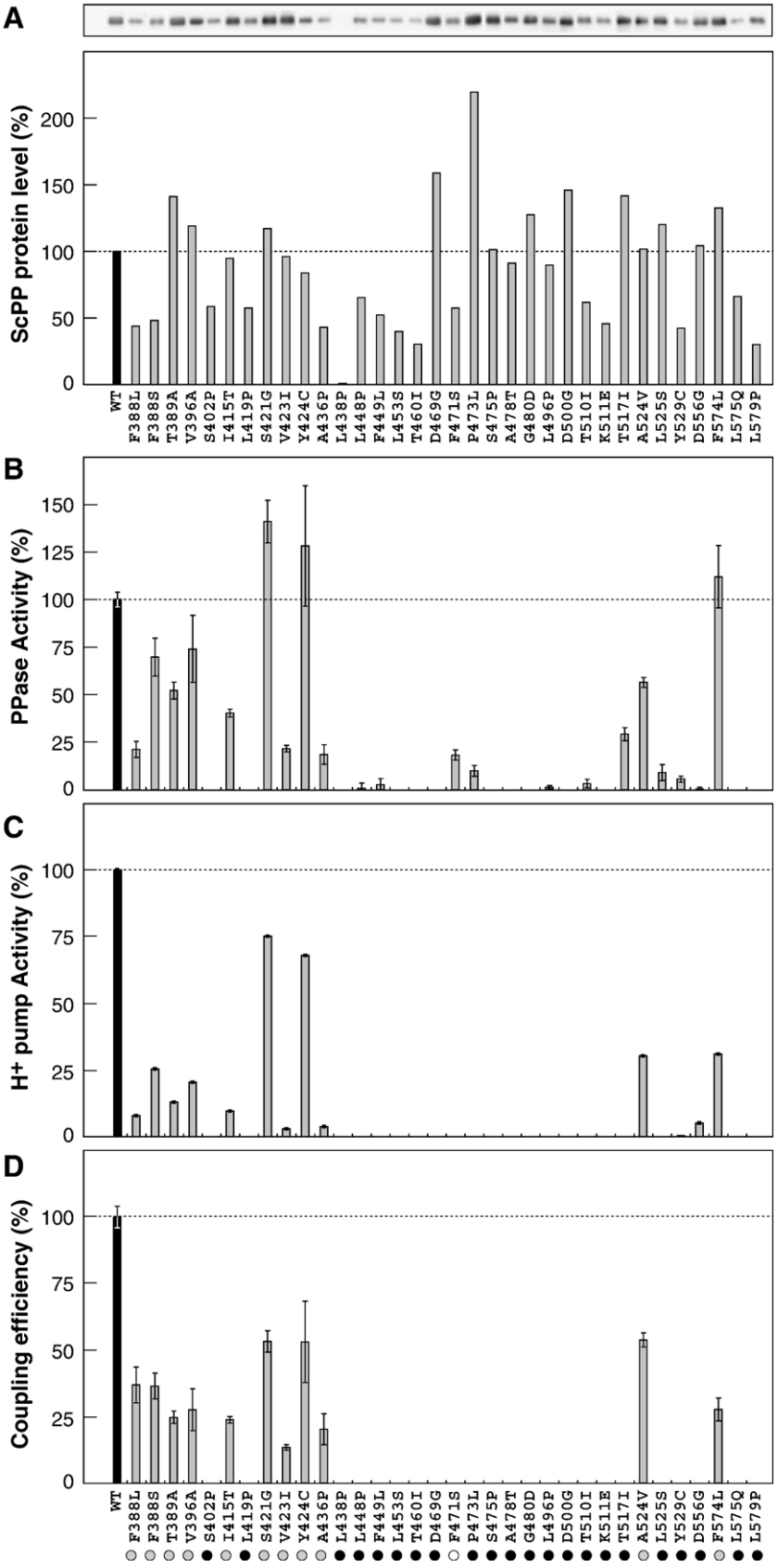

We selected mutants that had low activity (less than 70% of the WT enzyme) of PPase and H^+-pump for functional analysis. Mutants that had a decreased energy-coupling efficiency (that is, the relative ratio of H^+-pump activity to PPase activity) were also selected. The latter included mutants with normal PPase activity but decreased H^+-pump activity and mutants with decreased PPase activity and no H^+-pump activity. Totally 162 mutants with dysfunction were selected and sequenced. These mutants had various types of mutation: namely, single-site mutation (34 mutants), multi-site mutation (two sites, 40 mutants; three sites, 8 mutants, and more than four sites, 2 mutants), and silent mutation (5 mutants). The others were mutants with a frame shift caused by single-base deletion or with no mutation. A few mutants were overlapped. The presence of clones with no mutations is reasonable, since the mutation frequency of the library was 0.4 nucleotide change per clone. In this experiments we did not sequence the DNA of mutants except for 162 mutants mentioned above. Probably, other mutants with relatively high enzyme activity had silent mutations or non-effect mutations. We therefore selected 34 single mutants for further analysis, some of which contained silent mutations (Table 1).

3.2. Mutant ScPP expression and enzyme activity

The protein levels of mutant ScPPs were determined by immunoblotting with an anti-His_6 antibody. Addition of the C terminus His_6 tag to wild-type (WT) ScPP has previously been shown to have no effect on PPase and H^+-pump activities [28]. All of the mutants, except for L438P, accumulated in *E. coli* membranes at a level similar to the WT enzyme (Fig. 1A). Bands of 80 kDa were detected for all of the mutant and WT enzymes, suggesting that no proteolytic cleavage or covalent modification had occurred in the mutants.

Fig. 1B and C shows the activities of PPase and H^+-pump of the mutants. We also calculated the ratio of H^+-pump activity to PPase activity, in order to evaluate the energy-coupling efficiency of the mutants, and expressed it as a percentage of the value for the WT enzyme. The mutants could be divided into three groups; the "loose-coupling" group comprised of 11 mutants (F388L, F388S, T389A, V396A, I415T, S421G, V423I, Y424C, A436P, A524V, and F574L) which retained relatively high PPase activity but H^+-pump activity that was not in parallel with their PPase activity and coupling efficiency 13–54% of that of the WT enzyme, the "pump-less" group comprised of the F471S mutant which had only 18% of the PPase activity of the WT enzyme and no H^+-pump activity, and the "no activity" group comprised of 22 mutants having PPase activity less than 10% of that of WT and no H^+-pump activity. It should be noted that there was no marked difference in proton leakiness among the membrane vesicles prepared from cells expressing mutant ScPP such as V396A and the original *E. coli* cells. Thus the proton pump activity reflects the actual activity of proton translocation of each mutant enzyme.

Each mutation site of the random mutants is mapped in the membrane topology model (Fig. 2). The sites of 16 of 34 mutants were distributed throughout TM9 to TM13. The other mutation sites were located in hydrophilic loops. Several residues in the TMs of the third quarter of ScPP are conserved in the H^+-PPases of various organisms (Fig. 3). Random mutagenesis revealed that the conserved residue Leu^{525} in TM10 and the eight conserved residues in the cytoplasmic loops, Ser^{402}, Asp^{469}, Pro^{473}, Ser^{475}, Ala^{478}, Gly^{480}, Asp^{500}, and Lys^{511}, are essential for function. Our findings revealed that mutations at the other five conserved residues and 18 non-conserved residues affect the coupling ratio (Fig. 2). Thus, screening of random mutants is useful to identify unexpected residues that participate in enzyme functions.

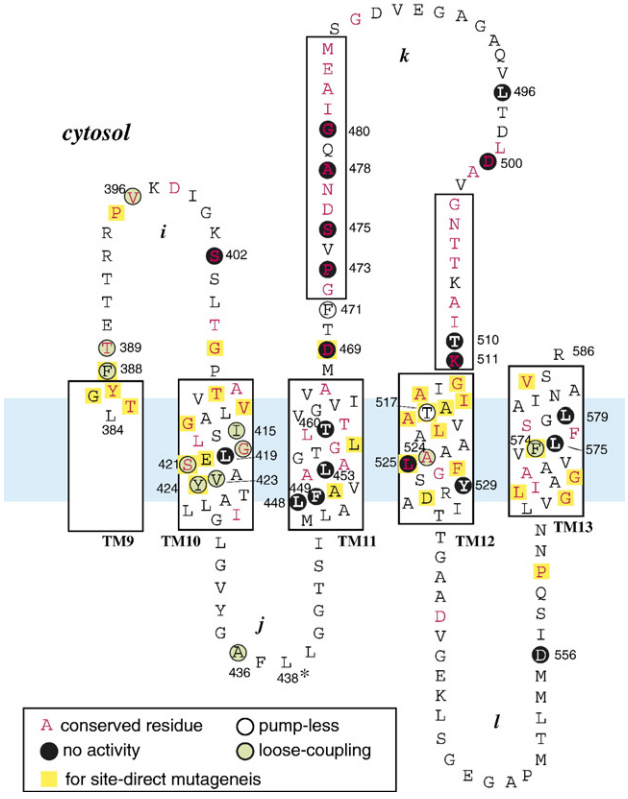

Fig. 2. Mutation sites of ScPP mutants in the topology model. Mutation sites of the third quarter of the ScPP sequence (TM9 to TM13) are mapped in the membrane topology model of ScPP [28]. Two boxes in the loop *k* indicate highly conserved motifs (see Fig. 3). Mutant ScPPs are categorized to three groups and marked separately. The numbers beside the residues show the positions of the mutation sites. Highly conserved residues are shown in red. L438P mutant marked with an asterisk was not accumulated in *E. coli* cells. Residues of the site-directed mutants are shown in yellow boxes (see text for details).

3.3. Site-directed mutation of ScPP

We further examined the effects of amino-acid replacements at single sites in the region from TM9 to TM13 with consideration of conserved residues as shown in Fig. 3, which shows sequence alignment of 12 organisms. We selected 32 sites for site-directed mutagenesis (Fig. 2), which included the conserved acidic residues in TMs (Glu^{420} and Asp^{531}) and conserved proline residues in hydrophilic loops (Pro^{395} and Pro^{560}). Also, the remaining residues, except for Tyr^{424}, are conserved among H^+-PPases. We examined the role of Glu^{420} and Asp^{531}, which were excluded from the random mutagenesis

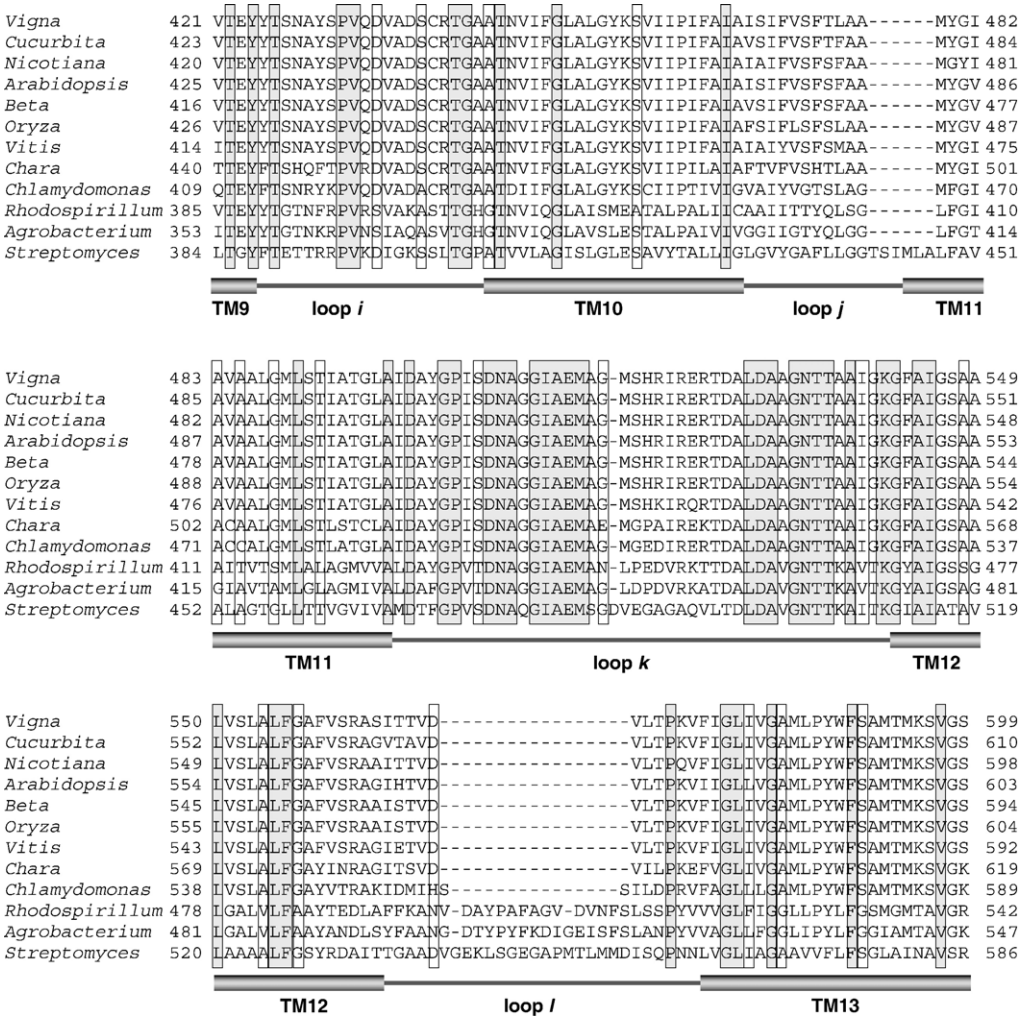

Fig. 3. Multiple alignment of the third quarter of ScPP with H^+-PPases from various organisms. TMs (TM9 to TM13) and loops (*i* to *l*) are shown as thick and thin bars, respectively, under the sequences. The accession numbers of sequences are: *Vigna radiata* (AB009077), *Cucurbita moschata* (BAA33149), *Nicotiana tabacum* (Q43798), *A. thaliana* (P31414), *Beta vulgaris* (AAA61609), *Oryza sativa* (BAA08232), *Vitis vinifera* (AAF69010), *Chara corallina* (AB018592, BAA36841), *Chlamydomonas reinhardtii* (CAC44451), *R. rubrum* (AAC38615), *Agrobacterium tumefaciens* (AAK86977), and *S. coelicolor* A3(2) (Q9X913). Identical residues are boxed and shaded. Highly conserved residues (identity with more than 75%) are boxed.

analysis, since acidic residues in the TMs are generally thought to play essential roles in proton transport. Although this Tyr^{424} is not conserved among H^+-PPases, the mutation Y424C, like S421G, resulted in imbalanced activity with relatively high PPase activity (Fig. 1). In total, 26 residues selected for the site-directed mutagenesis are in the TMs, three (Phe^{388}, Pro^{395}, and Gly^{406}) are in loop *i*, one (Gln^{469}) in loop *k*, and one (Pro^{560}) in loop *l* (Fig. 4).

3.4. Enzyme activities of site-directed ScPP mutants

In total, 31 residues were replaced individually by alanine or a related amino acid. We finally produced 39 site-directed mutant ScPPs and expressed them in *E. coli*. The mutant ScPP proteins were expressed in *E. coli*, as detected by immunoblotting (Fig. 4A). All mutants were expressed sufficient level for enzyme assay.

Fig. 4B and C shows the effect of amino-acid substitutions on PPase and H^+ pump activities, respectively. In total, nine mutants (P395A, G406A, T409A, V411A, G414A, D469A, D469E, D469N, and G569A) lost PPase activity, and the PPase activity of L525A was reduced to 24% of that of the WT. These results suggest that at least five residues (Thr^{409}, Val^{411}, Gly^{414}, Leu^{525}, and Gly^{569}) are strictly required for PPi hydrolysis, even though they are located in the TMs. The mutation of two residues in the cytoplasmic loops (Gly^{406} and Asp^{469}) also resulted in a complete loss of activity. These residues were positioned near TMs.

Judging from the results shown in Figs. 1 and 4, the substitution of Thr^{517}, Gly^{565}, Leu^{566}, and Val^{584} did not markedly affect enzyme activity. The effect of a substitution depends on the type of amino-acid residue substituted. This is relevant for Gly^{386} (alanine or glutamic acid), Phe^{388} (alanine, serine or leucine), Glu^{420} (alanine, glutamine or aspartic acid), Ser^{421} (alanine or glycine), Tyr^{424} (cysteine, alanine, phenylalanine or isoleucine), Asp^{469} (alanine, asparagine or glutamic acid), Thr^{517} (alanine or serine), Leu^{525} (alanine or serine) and Phe^{574} (leucine or alanine), and is discussed further later.

The energy-coupling efficiencies of ScPP mutants were calculated as shown in Fig. 4D. Sixteen of the 39 site-directed mutants were classified into the "no activity" (9 mutants), "pump-less" (1), and "loose-coupling" (6) mutants, as described for the random mutants. Nine mutants (F388A, E420Q, Y424A, Y424F, T517A, T517S, G565A, L566A, and V584A), with

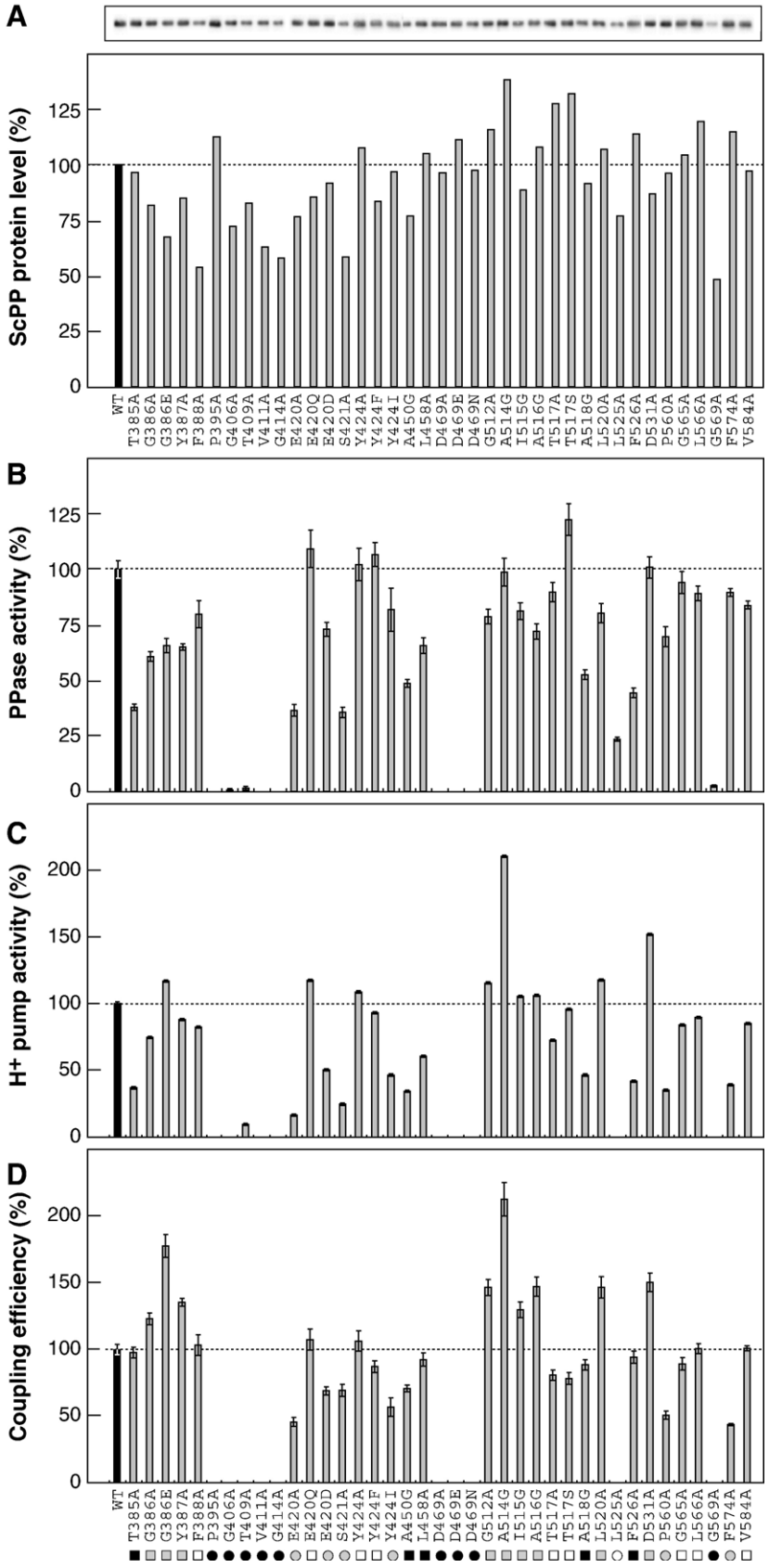

PPase and H^+-pump activities that were not affected were designated as "no effect" mutants. Five mutants (T385A, A450G, L458A, A518G, and F526A) that had low PPase and H^+-pump activities although their coupling efficiencies were normal were categorized as "low activity" mutants. The remaining nine mutants (G386A, G386E, Y387A, G512A, A514G, I515G, A516G, L520A, and D531A) that had a relatively high ratio of H^+ pump activity to PPase activity (the coupling ratio, >120%) were categorized as "high-pumping" mutants.

3.5. Enzymatic properties of "high-pumping" mutants

A total of 73 mutants with a single amino acid replacement by random or site-directed mutagenesis were examined for their activities and estimated coupling efficiency (Figs. 1 and 4). In several mutant categories, we focused on the "loose-coupling" and "high-pumping" groups, which showed a less and enhanced coupling ratio, respectively. We prepared typical mutants, V396A and F574L from "loose-coupling" and D531A from "high-pumping" mutants, and determined their activities. These proteins were reproducibly accumulated and expressed PPase activity, which were equivalent to that of the WT (data not shown). There were no marked differences in the levels and activity with the culture. We examined the WT and the mutants for PPase activity at different substrate concentrations. As shown in Fig. 5, the WT and mutant ScPPs showed sigmoid curves, but do not follow the hyperbolic Michaelis–Menten relationship. This might reflect cooperative interaction between subunits in the homodimer of H^+-PPases at low concentrations of substrate [1, 29]. The substrate concentrations giving half-maximal velocity, $K_{0.5}$ values, of WT and D531A mutant enzymes for Mg_2PPi, which is the actual substrate for H^+-PPase [35], were 13 and 17 μM, respectively. Thus, there was no marked difference in the values between WT and the mutant.

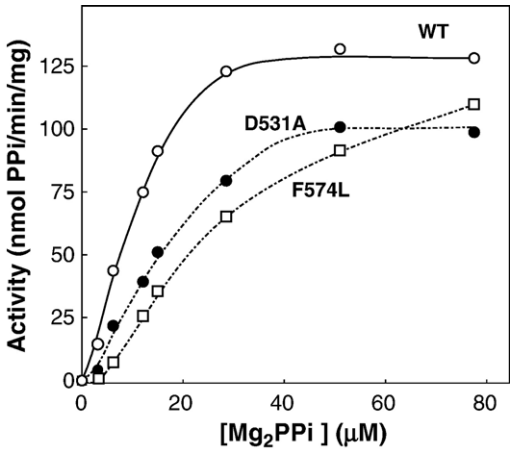

Fig. 5. Affinity of mutant enzymes for Mg_2PPi. Membrane preparations from two independent cultures of each *E. coli* strain expressing WT or mutant ScPP were assayed for ScPP protein level and enzyme activity. PPase activities of WT, F574L ("loose-coupling" mutant), and D531A ("high-pumping" mutant) were 129, 110, and 102 nmol PPi/min/mg protein, respectively. H^+-pump activities of WT, F574L, and D531A were 55, 20, and 66%Δ*F*/min/mg protein, respectively. Coupling efficiency was calculated as the ratio of H^+-pump activity to PPi hydrolysis activity (F574L, 42%; D531A, 152%). Then PPase activity was measured at different concentrations of Mg_2PPi. The Mg_2PPi complex concentration was calculated from the total concentration of Na_4PPi, 1 mM Mg^{2+}, and 100 mM K^+ at pH 8.0 [35].

4. Discussion

To elucidate the proton transport pathway of H^+-PPase, and the coupling mechanism between PPi hydrolysis and H^+ translocation, we performed a series of random mutagenesis analysis of the H^+-PPase of *S. coelicolor* A3(2) H^+-PPase. Site-directed mutagenesis has successfully determined the essential residues for the binding and hydrolysis of the substrate, and has provided critical information on the structure–function relationship of the cytoplasmic catalytic domain and a few TMs [3,4,20,22–28,38–40]. Site-directed mutagenesis is effective for evaluating specific residues and random mutagenesis is also effective for finding unexpected functional residues. In the present study, we focused the third quarter region (Leu^{384} to Arg^{586}) of ScPP and analyzed by random and site-directed mutagenesis. The third quarter region has highly conserved motifs in cytoplasmic loop *k*, which have been demonstrated to be essential for PPase activity by site-directed mutagenesis [3,4]. Random mutagenesis revealed several unexpected residues that were involved in active proton transport and energy transfer. The results of the random and site-directed mutagenesis are summarized in the helical wheels (Fig. 6) and the membrane topology model (Fig. 7). These functional residues were found in the cytoplasmic loops, periplasmic (intravacuolar) loops, and TMs. We discuss them separately below.

4.1. Residues in the cytosolic loops

Fig. 7 summarized the results of functional analysis on 73 mutants in 53 sites in the membrane topology model. The loop *k* has two motif sequences conserved in H^+-PPases: GPVSDNAQGIAEM and GNTTKAITK [3,4]. Two other conserved residues in this loop (Asp^{469} and Lys^{511}) were demonstrated to be essential for enzyme function as reported previously [21,26]. There is a possibility that these two charged residues form an ionic pair to maintain the structure as

Fig. 4. Expression levels and enzyme activities of site-directed mutants of ScPP. (A) Membrane vesicles were prepared from *E. coli* cells expressing WT and site-directed mutants as indicated. Membranes (5 μg) were subjected to immunoblotting with anti-His_6 antibodies (upper panel). The intensities of immunostained bands were quantified, and are expressed relative to that of WT (lower panel). (B) PPase activities of WT and mutant ScPPs are expressed relative to that of WT (81 nmol PPi/min/mg protein). (C) H^+-pump activities of WT and mutants are expressed relative to that of WT (85%Δ*F*/min/mg protein). (D) Coupling efficiencies were calculated as the ratios of H^+-pump activities to H^+-pump activities, and are expressed relative to that of WT. Mutant ScPPs are categorized as "no activity" (black circles), "pump-less" (open circles), and "loose-coupling" mutants (grey circles) as for the random mutants shown in Fig. 1. Mutants with coupling efficiencies of >70% are categorized as "low activity" mutants (black squares) and of <70% are categorized as "loose-coupling" mutants. Mutants with normal activities are designated "no effect" mutants (open squares). Mutants with coupling efficiencies of >120% are designated as "high-pumping" (grey squares).

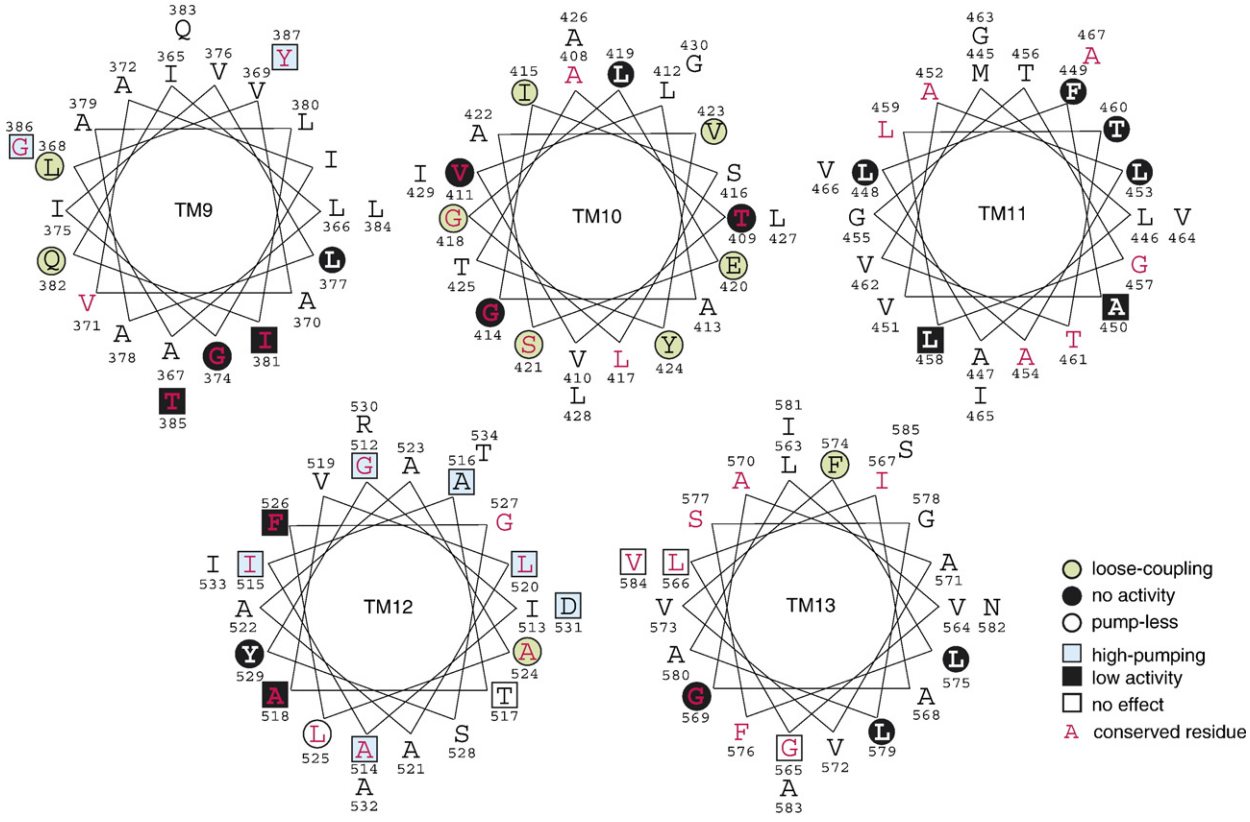

Fig. 6. Helical wheel models of the TM9 to TM13 segments. Amino-acid residues located in TMs are plotted on helical wheels. Conserved residues are shown in red.

demonstrated for the pair of Glu^{427} and Lys^{461} of *Arabidopsis* enzyme [41]. The present random mutagenesis study showed that seven residues in loop *k*, Pro^{473}, Ser^{475}, Ala^{478}, Gly^{480}, Leu^{496}, Asp^{500}, and Thr^{510}, were essential for PPase activity (Fig. 2). In addition, amino acid substitution of Pro^{395}, Ser^{402} and Gly^{406} in loop *i* resulted in "no activity" enzyme, suggesting these were involved in PPi hydrolysis. Eight of these 10 residues in cytosolic loops *i* and *k* are conserved among H^+-PPases. Thus, we concluded that these common residues play a key role in enzyme catalysis.

It should be noted that at least three mutations (F388S, T389A, and V396A) in the loop *i* are critical for enzyme function, especially H^+ transport and/or energy transfer. These three "loose-coupling" mutants retained >50% of PPi-hydrolysis activity and only 26% of proton-transport activity. Three residues (Pro^{395}, Ser^{402}, and Gly^{406}) in loop *i* were involved in the PPi hydrolysis as mentioned above. The energy-transfer mechanism from PPi hydrolysis might be impaired in these three "loose-coupling" mutants (F388S, T389A, and V396A). The present study revealed the functionality of loop *i* including five conserved residues (Phe^{388}, Thr^{389}, Pro^{395}, Val^{396}, Ser^{402}, and Gly^{406}).

4.2. Residues in the periplasmic loops

In the periplasmic loops, which correspond to the intravacuolar loops of plant H^+-PPases, three amino acid residues (Ala^{436}, Asp^{556}, and Pro^{560}) affected enzyme activity by replacement. P560A mutant retained >70% of PPase activity and only 40% of proton-pumping activity (Fig. 3). Because it is hard to assume direct effect of residues in periplasmic loops on PPi hydrolysis, this residue is related to energy conversion and/or proton translocation at a minimum and the replacement resulted in impairment of these functions. Pro^{560} of ScPP is a conserved residue and its location is common in plants and *R. rubrum* H^+-PPases [21,22,26]. Thus, this residue might play a common role, especially for accurate formation of the structure of this loop. In addition to conserved Pro^{560}, replacement of non-conserved residues, Ala^{436} and Asp^{556} of ScPP, had critical effect on the PPase activity. From this result and previous observation on Pro^{189}, Lys^{190}, Asp^{281}, Val^{351}, and Ala^{357} [31] (summarized in Fig. 7), it is estimated that the periplasmic loops are involved in the energy-coupling process and/or proton translocation including the release of proton from the enzyme.

4.3. Functional residues in TMs

Amino-acid substitution in the TMs impaired proton translocation and energy coupling. Sixteen residues (Thr^{409}, Val^{411}, Gly^{414}, Leu^{419}, Leu^{448}, Phe^{449}, Leu^{453}, Thr^{460}, Thr^{517}, Ala^{518}, Leu^{525}, Phe^{526}, Tyr^{529}, Gly^{569}, Leu^{575} and Leu^{579}) proved to be essential for PPi hydrolysis and proton-pump activity (Fig. 1 and 4). These residues except for threonine are non-polar neutral amino acids. Therefore, these residues may be essential for correct interaction between transmembrane helices. Furthermore, it is thought that five aromatic residues (Tyr^{424},

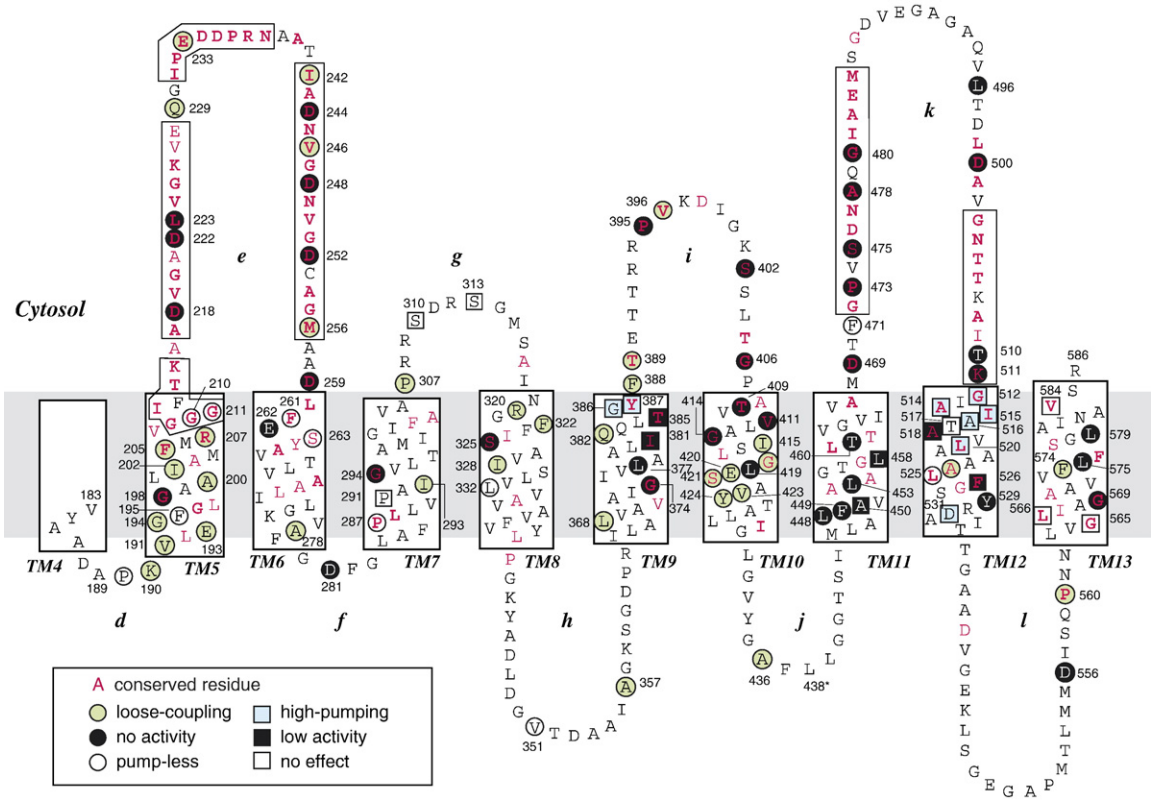

Fig. 7. Topological arrangement of mutation sites and effects of the mutations on enzyme activities. The results from the present analysis of the third quarter (Leu^{384} to Arg^{588}) are shown with the results of the previous study on the second quarter [31] in the membrane topology model of ScPP [28]. Mutant ScPPs are categorized as "no activity" (black circles), "pump-less" (open circles), "loose-coupling" (green circles), "low activity" (closed squares), "no effect" (open squares), and "high-pumping" mutants (light blue squares). Highly conserved residues are shown in red, and the highly conserved motifs in loop *e* and *k* are boxed. The numbers beside each residue shows the position of the mutation site.

Phe^{449}, Phe^{526}, Tyr^{529}, and Phe^{574}) interact with other aromatic residues and are involved in strengthening the helix–helix interaction between TMs.

In general, pairs of G*XXX*G sequences permit close packing of transmembrane helices because hydrogen bonds are formed between backbone carbonyls and the Cα hydrogens of glycine residues [42, 43]. ScPP has a total of four G*XXX*G sequences in TM5 (G*FGL*G), TM10 (G*ISL*G), TM13 (G*LIA*G), and TM14 (G*FTL*G). At least the two glycines of the GFGLG sequence in TM5 are essential for efficient coupling [31]. The present study revealed that Gly^{414} and Gly^{418} of GISLG in TM10 and Gly^{569} of GLIAG in TM13 are conserved residues and critical for enzyme function. However, mutation of Gly^{565} in TM13 with alanine residue had no effect on enzyme activity. The GFGLG sequence in TM5 might therefore interact with TM10 (GISLG) or TM14 (GFTLG).

ScPP has four acidic residues in TMs (Glu^{193}, Glu^{262}, Glu^{420}, and Asp^{531}). Amino acid replacement of Glu^{193} and Glu^{262} had been reported to be critical for enzyme function [31]. These two residues are not conserved among H^+-PPases, however glutamate or aspartate residue exists near these sites. Therefore Glu^{193} and Glu^{262} may be directly involved in proton translocation as common residues in TM5 and TM6s. The other two residues, Glu^{420} and Asp^{531}, are conserved in H^+-PPases of only *R. rubrum* and *A. tumefaciens* (Fig. 3). There is no acidic residue around these sites of plant H^+-PPase. Nevertheless, their amino-acid replacement changed the activity markedly (Fig. 4). E420A and E420D had low activity, and E420Q had full activity. Thus, the side-chain structure of glutamic acid, probably carbonyl oxygen, might be important than its negative charge. D531A was a "high-pumping" mutant. Thus, it is suggested that Glu^{420} and Asp^{531} are characteristic residues of *R. rubrum*, *A. tumefaciens*, and *S. coelicolor* A3(2) H^+-PPases and play a role in the regulation of proton transport and/or energy transduction in TMs.

4.4. "High-pumping" mutants

Site-directed mutagenesis generated eight "high-pumping" mutants (Fig. 4). These mutation sites, except for Asp^{531}, were located in the cytoplasmic half of TM9 and TM12 (Fig. 7). Four residues (Gly^{512}, Ile^{515}, Ala^{516}, and Leu^{520}) are clustered on a half side of the helical wheel of TM12 (Fig. 6), and linked to the conserved motif in loop *k*. In these mutants, the residues were replaced with small side-chain residue, alanine or glycine. TM12 including these residues may participate in hydrophobic interaction between helices to support the functional loop *k* and is essential for determination of the stoichiometry of H^+ to PPi during the reaction. The H^+/PPi ratio of plant vacuolar H^+-PPase has been reported to be 1:1 [44]. For "high-pumping"

mutants, the H^+/PPi stoichiometry possibly increases from 1 to 2. If it is the case, the energy-coupling efficiency may be two-fold of the WT enzyme. In case of mutant ScPPs, both PPase and proton pump activities might be affected by amino acid substitution and the energy-coupling values varied with the mutants. This is the first observation of the mutant H^+-PPase with enhanced ratio of proton pump activity to PPase activity. Especially TM9 and TM12 play crucial role on the energy-coupling efficiency. Further detailed analysis will be needed to obtain the H^+/PPi stoichiometry of the mutant ScPPs.

The PPase activity of G386E was only 65% of that of the WT enzyme and the coupling efficiency was 176% (Fig. 4). The site of Gly^{386} in TM9 is occupied by the glutamic-acid residue in H^+-PPases of all organisms except for *Streptomyces* (Fig. 3). For example, Glu^{427} of *Arabidopsis* enzyme is located to the site of Gly^{386} of ScPP. In the case of Glu^{427} of *Arabidopsis* H^+-PPase, E427D had the same PPase activity as the WT and enhanced H^+-pump activity (135% of the WT enzyme) [21]. Therefore, this position corresponding to Gly^{386} of ScPP and Glu^{427} of *Arabidopsis* enzyme is a topological key site for energy coupling. In relation to the exchange of amino acid residue of ScPP with the other one conserved in other H^+-PPases, we obtained a "high-pumping" mutant of A516G. Ala^{516} in TM12 is unique to ScPP and this site is occupied with glycine in other PPases (Fig. 3). Substitution of Ala^{516} with glycine increased the H^+ pumping activity. An artificial H^+-PPase with high energy-coupling efficiency could be generated by replacing the ScPP-specific residue with another residue conserved in other H^+-PPases, as in G386E and A516G. The presence of "high-coupling" artificial variants suggests a possibility that the H^+/PPi stoichiometry of H^+-PPase in living organisms might be suppressed to 1.

In conclusion, we identified essential residues in the transmembrane helices from TM9 to TM13 and in loops *i* and *k*. Three functional residues were also found in the periplasmic loops *j* and *l*. These residues are essential for efficient H^+ translocation and energy coupling not only in the TMs but also in the hydrophilic loops. At present, it is difficult to distinguish the direct and indirect effects of amino acid substitution and to determine the topological arrangement of mutation sites in the tertiary structure of H^+-PPase. From the results of present and previous studies, we made a distribution map of essential residues in the central half region of ScPP (404 of 794 residues). Furthermore, the present study revealed that substitution of several residues in the TMs had a positive effect on the energy coupling efficiency. How the H^+-PPases in living cells are kept at the H^+/PPi ratio of 1 remains an issue for the future.

Acknowledgements

This work was supported by Grants-in-Aid for Scientific Research 16085204, 18380064, and 19042012 from the Ministry of Education, Sports, Culture, Science and Technology of Japan, the Program for Promotion of Basic Research Activities for Innovative Biosciences of Japan (PROBRAIN), and the Global Research program of the Ministry of Science and Technology of Korea (to M.M.).

References

[1] M. Maeshima, Vacuolar H^+-pyrophosphatase, Biochim. Biophys. Acta 1465 (2000) 37–51.
[2] M. Baltscheffsky, S. Nadanaciva, A. Schultz, A pyrophosphate synthase gene: molecular cloning and sequencing of the cDNA encoding the inorganic pyrophosphate synthase from *Rhodospirillum rubrum*, Biochim. Biophys. Acta 1364 (1998) 301–306.
[3] M. Baltscheffsky, A. Schultz, H. Baltscheffsky, H^+-PPases: a tight membrane-bound family, FEBS Lett. 457 (1999) 527–533.
[4] Y.M. Drozdowicz, A. Rea, Vacuolar H^+-pyrophosphatases: from the evolutionary backwaters into the mainstream, Trends Plant Sci. 6 (2001) 206–211.
[5] M. Maeshima, S. Yoshida, Purification and properties of vacuolar membrane proton-translocating inorganic pyrophosphatase from mung bean, J. Biol. Chem. 264 (1989) 20068–20073.
[6] Y. Nakanishi, N. Matsuda, K. Aizawa, T. Kashiyama, K. Yamamoto, T. Mimura, M. Ikeda, M. Maeshima, Molecular cloning of the cDNA for vacuolar H^+-pyrophosphatase from *Chara corallina*, Biochim. Biophys. Acta 1418 (1999) 245–250.
[7] D.A. Scott, W. de Souza, M. Benchimol, L. Zhong, G.G. Lu, S.N.J. Moreno, R. Docampo, Presence of a plant-like proton-pumping pyrophosphatase in acidocalcisomes of *Trypanosoma cruzi*, J. Biol. Chem. 273 (1998) 22151–22158.
[8] C.R. Garcia, H. Celis, I. Romero, Importance of *Rhodospirillum rubrum* H^+-pyrophosphatase under low-energy conditions, J. Bacteriol. 186 (2004) 6651–6655.
[9] M. Seufferheld, C.R. Lea, M. Vieira, E. Oldfield, R. Docampo, The H^+-pyrophosphatase of *Rhodospirillum rubrum* is predominantly located in polyphosphate-rich acidocalcisomes, J. Biol. Chem. 279 (2004) 51193–51202.
[10] Y.M. Drozdowicz, Y.P. Lu, V. Patel, S. Fitz-Gibbon, J.H. Miller, P.A. Rea, A thermostable vacuolar-type membrane pyrophosphatase from the archaeon *Pyrobaculum aerophilum*: implications for the origins of pyrophosphate-energized pumps, FEBS Lett. 460 (1999) 505–512.
[11] M. Seufferheld, M.C.F. Viera, F.A. Ruiz, C.O. Rodrigues, S.N.J. Moreno, R. Docampo, Identification of organelles in bacteria similar to acidocalcisomes of unicellular eukaryotes, J. Biol. Chem. 278 (2003) 29971–29978.
[12] R.A. Gaxiola, J. Li, S. Undurraga, L.M. Dang, G.J. Allen, S.L. Alper, G.R. Fink, Drought- and salt-tolerant plants result from overexpression of the AVP1 H^+-pump, Proc. Natl. Acad. Sci. U. S. A. 98 (2001) 11444–11449.
[13] J. Li, H. Yang, W.A. Peer, G. Rchter, J. Blakeslee, A. Bandyopadhyay, B. Titapiwantakun, S. Undurraga, M. Khodakovskaya, E.L. Richards, B. Krizek, A.S. Murphy, S. Gilroy, R. Gaxiola, *Arabidopsis* H^+-PPase AVP1 regulates auxin-mediated organ development, Science 310 (2005) 121–125.
[14] Y. Nakanishi, M. Maeshima, Molecular cloning of vacuolar H^+-pyrophosphatase and its developmental expression in growing hypocotyls of mung bean, Plant Physiol. 116 (1998) 589–597.
[15] C. Bremberger, U. Lüttge, Dynamics of tonoplast proton pumps and other tonoplast proteins of *Mesembryanthemum crystallinum* L. during the induction of crassulacean acid metabolism, Planta 188 (1992) 575–580.
[16] S. Park, J. Li, J.K. Pittman, G.A. Berkowitz, H. Yang, S. Undurraga, J. Morris, K.D. Hirschi, R.A. Gaxiola, Up-regulation of a H^+-pyrophosphatase (H^+-PPase) as a strategy to engineer drought-resistant crop plants, Proc. Natl. Acad. Sci. U. S. A. 102 (2005) 18830–18835.
[17] R.L. López-Marqués, J.R. Pérez-Castiñeira, M. Losada, A. Serrano, Differential regulation of soluble and membrane-bound inorganic pyrophosphatases in the photosynthetic bacterium *Rhodospirillum rubrum* provides insights into pyrophosphate-based stress bioenergetics, J. Bacteriol. 186 (2004) 5418–5426.
[18] K.J. Saliba, R.J.W. Allen, S. Zissis, P.G. Bray, S.A. Ward, K. Kirk, Acidification of the malaria parasite's digestive vacuole by a H^+-ATPase and a H^+-pyrophosphatase, J. Biol. Chem. 278 (2003) 5605–5612.
[19] G. Lemercier, S. Dutoya, S. Luo, F.A. Ruiz, C.O. Rodrigues, T. Baltz, R. Docampo, N. Bakalara, A vacuolar-type H^+-pyrophosphatase governs maintenance of functional acidocalcisomes and growth of the insect and mammalian forms of *Trypanosoma brucei*, J. Biol. Chem. 277 (2002) 37369–37376.

[20] E.J. Kim, R.G. Zhen, P.A. Rea, Site-directed mutagenesis of vacuolar H^+-pyrophosphatase: Necessity of Cys^{634} for inhibition by maleimides but not catalysis, J. Biol. Chem. 270 (1995) 2630–2635.
[21] R.G. Zhen, E.J. Kim, P.A. Rea, Acidic residues necessary for pyrophosphate-energized pumping and inhibition of the vacuolar H^+-pyrophosphatase by *N, N′*-dicyclohexylcarbodiimide, J. Biol. Chem. 272 (1997) 22340–22348.
[22] Y. Nakanishi, T. Saijo, Y. Wada, M. Maeshima, Mutagenesis analysis of functional residues in putative substrate-binding site and acidic domains of vacuolar H^+-pyrophosphatase, J. Biol. Chem. 276 (2001) 7654–7660.
[23] Y.Y. Hsiao, R.C. Van, S.H. Hung, H.H. Lin, R.L. Pan, Roles of histidine residues in plant vacuolar H^+-pyrophosphatase, Biochim. Biophys. Acta 1608 (2004) 190–199.
[24] R.C. Van, Y.J. Pan, S.H. Hsu, Y.T. Huang, Y.Y. Hsiao, R.L. Pan, Role of transmembrane segment 5 of the plant vacuolar H^+-pyrophosphatase, Biochim. Biophys. Acta 1709 (2005) 84–94.
[25] A.M. Malinen, G.A. Belogurov, M. Salminen, A.A. Baykov, R. Lahti, Elucidating the role of conserved glutamates in H^+-pyrophosphatase of *Rhodospirillum rubrum*, J. Biol. Chem. 279 (2004) 26811–26816.
[26] A. Schultz, M. Baltscheffsky, Properties of mutated *Rhodospirillum rubrum* H^+-pyrophosphatase expressed in *Escherichia coli*, Biochim. Biophys. Acta 1607 (2003) 141–151.
[27] G.A. Belogurov, R. Lahti, A lysine substitute for K^+: A460K mutation eliminates K^+ dependence in H^+-pyrophosphatase of *Carboxydothermus hydrogenoformans*, J. Biol. Chem. 277 (2002) 49651–49654.
[28] H. Mimura, Y. Nakanishi, M. Hirono, M. Maeshima, Membrane topology of the H^+-pyrophosphatase of *Streptomyces coelicolor* determined by cysteine-scanning mutagenesis, J. Biol. Chem. 279 (2004) 35106–35112.
[29] H. Mimura, Y. Nakanishi, M. Maeshima, Oligomerization of the H^+-pyrophosphatase and its structural and functional consequences, Biochim. Biophys. Acta 1708 (2005) 393–403.
[30] H. Mimura, Y. Nakanishi, M. Maeshima, Disulfide bond formation in the H^+-pyrophosphatase of *Streptomyces coelicolor* and its implication in redox control and structure, FEBS Lett. 579 (2005) 3625–3631.
[31] M. Hirono, Y. Nakanishi, M. Maeshima, Essential amino acid residues in the central transmembrane domains and loops for energy coupling of *Streptomyces coelicolor* A3(2) H^+-pyrophosphatase, Biochim. Biophys. Acta 1767 (2007) 930–939.
[32] R.D. Kirsch, E. Joly, An improved PCR-mutagenesis strategy for two-site mutagenesis or sequence swapping between related genes, Nucleic Acids Res. 26 (1998) 1848–1850.
[33] M.M. Bradford, A rapid and sensitive method for the quantitation of microgram quantities of protein utilizing the principle of protein-dye binding, Anal. Biochem. 72 (1976) 248–254.
[34] M. Hirono, H. Mimura, Y. Nakanishi, M. Maeshima, Enzymatic and molecular properties of H^+-pyrophosphatase of *Streptomyces coelicolor* expressed in *Escherichia coli*, J. Biochem. 138 (2005) 183–191.
[35] A.A. Baykov, N.P. Bakuleva, P.A. Rea, Steady-state kinetics of substrate hydrolysis by vacuolar H^+-pyrophosphatase: a simple three-state model, Eur. J. Biochem. 217 (1993) 755–762.
[36] A.B. Bennett, R.M. Spanswick, Optical measurements of ΔpH and $\Delta\psi$ in corn root membrane vesicles: kinetic analysis of Cl^- effects on a proton-translocating ATPase, J. Membr. Biol. 71 (1983) 95–107.
[37] E. Blumwald, P.A. Rea, R.J. Poole, Preparation of tonoplast vesicles: applications to H^+-coupled secondary transport in plant vacuoles, Methods Enzymol. 148 (1987) 115–123.
[38] G.A. Belgurov, M.V. Turkina, A. Penttinen, S. Huopalahti, A.A. Baykov, R. Lahti, H^+-pyrophosphatase of *Rhodospirillum rubrum*: high yield expression in *Escherichia coli* and identification of the Cys residues responsible for inactivation by mersalyl, J. Biol. Chem. 277 (2002) 22209–22214.
[39] Y. Nakanishi, I. Yabe, M. Maeshima, Patch clamp analysis of H^+ pump expressed in giant yeast vacuoles, J. Biochem. 134 (2003) 615–623.
[40] M. Maeshima, Tonoplast transporters: organization and function, Annu. Rev. Plant Physiol. Plant Mol. Biol. 52 (2001) 469–497.
[41] M. Zancani, L.A. Skiera, D. Sanders, Roles of basic residues and salt–bridge interaction in a vacuolar H^+-pumping pyrophosphatase (AVP1) from *Arabidopsis thaliana*, Biochim. Biophys. Acta 1768 (2007) 311–316.
[42] J.U. Bowie, Solving the membrane protein folding problem, Nature 438 (2005) 581–589.
[43] K. Liu, D. Kozono, Y. Kato, P. Agre, A. Hazama, M. Yasui, Conversion of aquaporin 6 from an anion channel to a water-selective channel by a single amino acid substitution, Proc. Natl. Acad. Sci. U. S. A. 102 (2005) 2192–2197.
[44] J.M. Davies, R.J. Poole, D. Sanders, The computed free energy change of hydrolysis of inorganic pyrophosphate and ATP: apparent significance for inorganic-pyrophosphate-driven reactions of intermediary metabolism, Biochim. Biophys. Acta 1141 (1993) 29–36.